Manipulating vortex motion by thermal and Lorentz force in high-temperature superconductors

Z. Wang, L. Shan, Y. Z. Zhang, J. Yan, F. Zhou, J. W. Xiong, W. X. Ti, and H. H. Wen*
National Laboratory for Superconductivity, Institute of Physics, Chinese Academy of Sciences, Beijing National Laboratory for Condensed Matter Physics, P.O. Box 603, Beijing, 100080, China
(Received 16 June 2005; published 9 August 2005)

By using thermal and Lorentz force, the vortex motion is successfully manipulated in the mixed state of underdoped $La_{2-x}Sr_xCuO_4$ single crystals and optimally doped $YBa_2Cu_3O_{7-\delta}$ thin films. A conclusion is drawn that the strong Nernst signal above T_c is induced by vortex motion. In the normal state, in order to reduce the dissipative contribution from the quasiparticle scattering and enhance the signal due to the possible vortex motion, a new measurement configuration is proposed. It is found that the in-plane Nernst signal ($H \| c$) can be measurable up to a high temperature in the pseudogap region, while the Abrikosov flux flow dissipation can only be measured up to T_c. This may point to different vortices below and above T_c if we attribute the strong Nernst signal in the pseudogap region to the vortex motion. Below T_c the dissipation is induced by the motion of the Abrikosov vortices. Above T_c the dissipation may be caused by the motion of the spontaneously generated unbinded vortex-antivortex pairs.

DOI: 10.1103/PhysRevB.72.054509 PACS number(s): 74.40.+k, 74.25.Fy, 74.72.Dn

I. INTRODUCTION

One of the core issues in a high-temperature superconductor is the origin of the pseudogap above T_c in the underdoped region. In order to understand the physics of the pseudogap, many theoretical models have been proposed, such as spin fluctuation,[1] preformed Cooper pair,[2,3] charge stripes,[4] *d*-density wave (DDW),[5,6] etc. Among many of them, the pseudogap state has been considered as the precursor to the superconducting state. In the pseudogap region above T_c, a significant in-plane Nernst signal has been discovered by Xu *et al.*[7] in the underdoped $La_{2-x}Sr_xCuO_4$ single crystal, and they attributed this signal to vortexlike excitations above T_c. This result has been confirmed in other families of cuprate superconductors.[8,9] By doing experiments with the magnetic field applied along different directions, Wen *et al.*[10] gave a strong indication for a two-dimensional (2D) feature of the Nernst effect in the pseudogap region of underdoped cuprate superconductors. About the origin of the strong Nernst signal above T_c, it remains highly controversial. Wang *et al.*[9,11] suggested that the large Nernst signal supports the scenario[2] where the superconducting order parameter disappears at a much higher temperature instead of T_c. Kontani[12] suggested that the pseudogap phenomena including the strong Nernst signal can be well-described in terms of the Fermi liquid with antiferromagnetic and superconducting fluctuations. Ussishkin *et al.*[13] proposed that the Gaussian superconducting fluctuations can sufficiently explain the Nernst signal in the optimally doped and overdoped region, but in the underdoped region the actual T_c is suppressed from mean-field temperature by non-Gassian fluctuation. Tan *et al.*[14] believed that a preformed-pair alternative to the vortex scenario can lead to a strong Nernst signal. Alexandrov and Zavaritaky[15] proposed a model based on normal state carrier without superconducting fluctuation, which, as they asserted, "can describe the anomalous Nernst signal in high-T_c cuprate."[15]

It is thus strongly desired to investigate the feature of Nernst signal below and above T_c. One possibility is that the strong Nernst signal above T_c is originated from or partly from the motion of vortex, but the structure and the feature of the vortices above T_c are different from those below T_c. We thus measured the in-plane Nernst voltage and the resistance of the underdoped $La_{2-x}Sr_xCuO_4$ single crystals and optimally doped $YBa_2Cu_3O_{7-\delta}$ thin films in the magnetic field perpendicular to the *ab*-plane. Besides the temperature gradient, we applied a transverse current to manipulate the possible motion of the vortices. Especially we measured the longitudinal voltage in a new configuration which may reduce the dissipative contribution from the quasiparticle scattering and enhance the signal due to the possible vortex motion. In this new configuration, a strong signal measured from the Nernst leads above T_c is observed in underdoped samples. The signal may be caused by the motion of quasiparticles and vortex. Our results indicate that the Nernst signal above T_c is contributed by vortex. The results were analyzed and we think that if a strong Nernst signal in the pseudogap region is contributed by the vortex motion, vortices are different below and above T_c. Below T_c the dissipation is induced by the motion of the Abrikosov vortices. Above T_c the dissipation may be caused by the motion of the spontaneously generated unbinded vortex-antivortex pairs (vortex plasma).

II. EXPERIMENTAL TECHNIQUES

The $La_{1.89}Sr_{0.11}CuO_4$ single crystals measured in this work were prepared by the traveling solvent floating-zone technique.[16] The perfect crystallinity of the single crystals was characterized by x-ray diffraction patterns.[16] The single crystal sample is shaped into a bar with the dimensions of 4.2 mm (length) $\times$ 1 mm (width) $\times$ 0.5 mm (thickness). The crystal along the length direction is [110]. The optimally doped $YBa_2Cu_3O_{7-\delta}$ thin films were prepared by coevaporation on MgO substrates with dimensions of 10 mm (length) $\times$ 1 mm (width), and the thickness of the film is about 5000 Å. We annealed the $YBa_2Cu_3O_{7-\delta}$ film to an underdop-

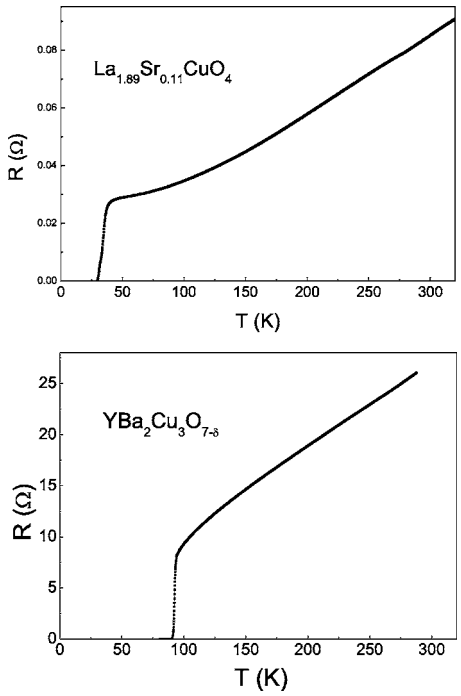

FIG. 1. Temperature dependence of resistance for $La_{1.89}Sr_{0.11}CuO_4$ single crystal (upper) and $YBa_2Cu_3O_{7-\delta}$ thin film (lower).

ing state and measured its Nernst voltage in the mixed and normal state. The resistance characteristics of the samples measured are shown in Fig. 1.

The measurement configuration in our experiment is illustrated in Fig. 2. The magnetic field is applied along the *c* axis of the samples. The $R(H)$ curves of the samples were obtained by the standard four-point method at different temperatures. A heater with a power of 1 mW (for the single crystal) or 9 mW (for the thin film) producing the thermal gradient is adhered on one end of the $YBa_2Cu_3O_{7-\delta}$ thin film sample (left) and $La_{1.89}Sr_{0.11}CuO_4$ single crystal sample (right). The other end of the sample is adhered on a cold sink. Along the direction E-F (perpendicular to the thermal gradient) the Nernst voltage signal V_N is measured. Two thermometers are attached onto the sample to detect the temperature gradient of the samples. In order to control the vortex motion by Lorentz force, we applied a direct transverse current of 3 mA along A-B and measured the longitudinal voltage between the points C and D. Since the dc current here can exert a Lorentz force to the vortices down or againt the thermal stream direction, the motion of the vortex can be manipulated by thermal and/or Lorentz force. All leads are sticked onto the samples by solidified silver paste at corresponding electrodes with the contact resistance below 0.1Ω. All measurements are based on an Oxford cryogenic system (Maglab-12) with temperature fluctuation less than 0.04% and magnetic fields up to 12 T. The Nernst voltage and the longitudinal voltage are measured by a Keithley 182-nanovoltmeter with a resolution of about 5 nV in the present case. During the measurement for Nernst and longitudinal voltage the magnetic field is applied parallel to the *c* axis and swept between 12 and −12 T. The Nernst signal V_N is obtained by subtracting the positive field value with the negative one in order to remove the Faraday signal during sweeping the field and the possible thermal electric power due to asymmetry of the electrodes. The Longitudinal signal V_L is obtained by averaging the data obtained from positive field and the negative field.

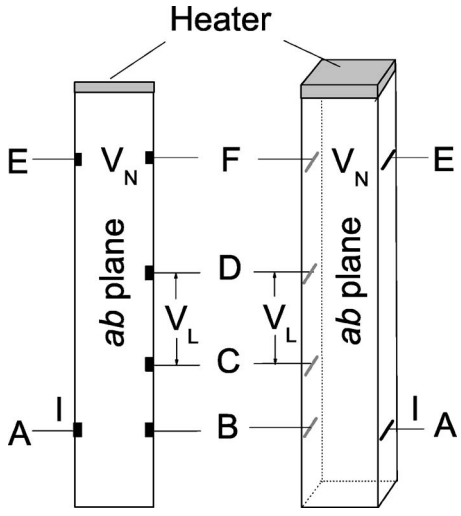

FIG. 2. The configuration for measuring the Nernst and longitudinal voltage of $La_{1.89}Sr_{0.11}CuO_4$ single crystal (right) and $YBa_2Cu_3O_{7-\delta}$ thin film (left). The Nernst voltages V_N can be obtained between E and F when the samples are heated by the heaters on one end and the longitudinal voltage V_L can be obtained between C and D when a dc current I is applied along the A-B direction.

III. RESULTS AND DISCUSSION

A. Pure Nernst signal

Figure 3 shows the Nernst voltage measured on the $La_{1.89}Sr_{0.11}CuO_4$ single crystal with a thermal gradient along the [110] (length) direction at temperatures from 5 to 180 K. In the low temperature region, the Nernst signal is dominated by the motion of Abrikosov vortices. One can see that the Nernst signal is precisely zero when the vortices are frozen in the case of 5, 10, and 15 K. The flow of vortices after melting leads to a Nernst signal increasing drastically with H. A strong in-plane Nernst signal resulting from vortices flow can also be seen in the curves for 20, 25, and 30 K, and can be measured far above T_c (29.3 K for our sample). When the temperature is above 80 K, the signal becomes negative and gradually approaches a background. When the temperature is above 150 K the Nernst signal becomes insensitive to temperature and does not change anymore with T. Similar results appear in the Nernst voltage measured on the underdoped $YBa_2Cu_3O_{7-\delta}$ thin film, though it is not as strong as that of $La_{1.89}Sr_{0.11}CuO_4$ single crystal sample. But no strong Nernst signal above T_c is observed in optimally doped $YBa_2Cu_3O_{7-\delta}$ thin film.

B. Flux flow resistance

Figure 4 shows the $R(H)$ curves of the $La_{1.89}Sr_{0.11}CuO_4$ single crystal at temperatures from 10 to 80 K measured by

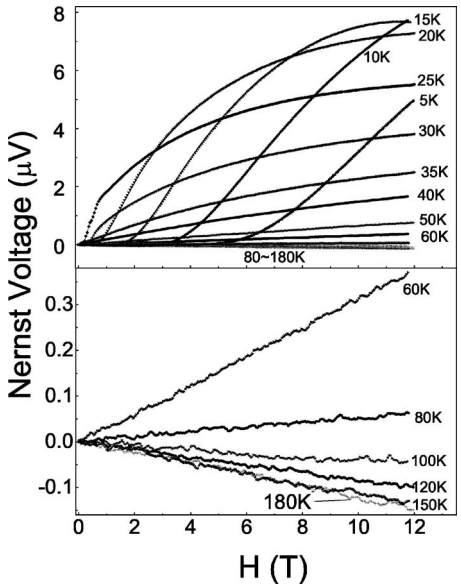

FIG. 3. Nernst voltage ($I=0$) of $La_{1.89}Sr_{0.11}CuO_4$ single crystal at temperatures from 5 to 180 K (upper panel). In order to make the result more obvious, the data in the high temperature region (from 60 to 180 K) are plotted in the lower panel. At temperatures of 5, 10, and 15 K, the vortices are frozen showing a background with precisely zero signal under relatively low field. A strong in-plane Nernst signal can be seen in the curves for 20, 25, and 30 K, and can be measured far above T_c. When the temperature is above 80 K, the signal becomes negative and gradually approaches a background. When the temperature is above 150 K the Nernst signal becomes insensitive to temperature and does not change anymore with T.

the standard four-point method. A zero resistance can be seen when the flux lattice is frozen at the low temperature of 10, 15, and 20 K. The Abrikosov flux flow dissipation after vortex melting can be seen in the higher temperature region. But the curvature due to the motion of Abrikosov vortices disappears when the temperature is above T_c. The dissipation becomes very weakly dependent on H in the normal state, which cannot be explained by the motion of Abrikosov vortices.

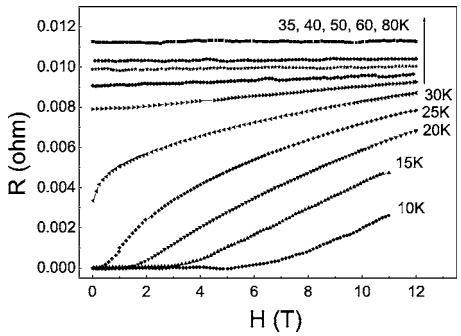

FIG. 4. H dependence of the resistance of $La_{1.89}Sr_{0.11}CuO_4$ single crystal at different fixed temperatures without thermal gradient. The Abrikosov flux flow dissipation can be seen below T_c, but the resistance is insensitive to H above T_c.

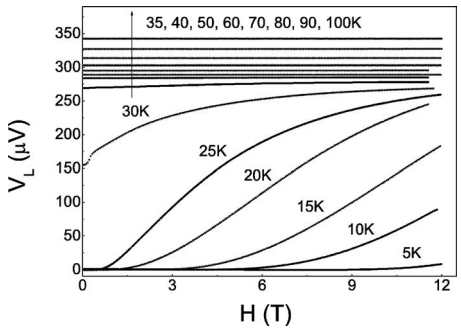

FIG. 5. H dependence of the longitudinal voltage of $La_{1.89}Sr_{0.11}CuO_4$ single crystal between the points C and D with a current of 3 mA between the points of A and B and without thermal gradient in the configuration shown in Fig. 2

C. Longitudinal signal

The dissipation shown above may be comprised of the contributions of both the flux flow and the quasiparticle scattering. The new configuration in our experiment can reduce the dissipative contribution from the quasiparticle scattering and enhance the signal due to the possible vortex motion if we send a current between A-B and measure the voltage between C-D. As shown in Fig. 2, the current was applied in the A-B direction, and the longitudinal voltage between the points on the side of the sample C and D was measured. As the C-D direction is perpendicular to the current direction and the two points are located outside the regime where the main current can reach, the voltage induced by the motion of quasiparticles is practically reduced; while the motion of the vortex crossing C-D induced by the current pump can be detected and are enhanced relatively as a consequence. The results of the longitudinal voltage measurement for underdoped single crystal at temperatures 5–100 K and optimally doped $YBa_2Cu_3O_{7-\delta}$ thin film at temperatures 72–100 K are shown in Figs. 5 and 6, respectively. We can see in both figures the similar dissipation manner as that of the resistance of the samples in magnetic field shown in Fig. 4. The dissipation deriving from the motion of Abrikosov vortices disappears when the temperature is above T_c, where the dis-

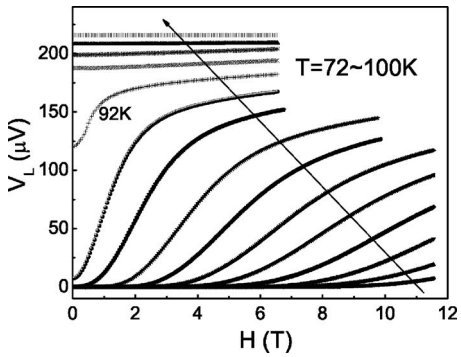

FIG. 6. H dependence of the longitudinal voltage of $YBa_2Cu_3O_{7-\delta}$ thin film between the points C and D with a current of 3 mA between the points of A and B and without thermal gradient in the configuration shown in Fig. 2. The step of temperature is 2 K.

sipation of the samples is independent on magnetic field at fixed temperatures.

The results from the measurement of Nernst voltage, resistance, and longitudinal voltage of our samples at different temperatures may indicate different vortices below and above T_c, provided that the dissipation is attributed to the vortex motion. Apparently, below T_c the dissipation is induced by the motion of the Abrikosov vortices. The Abrikosov vortex dissipation leads to the resistance in mixed state and, at the same time, the phase slip caused by the motion of Abrikosov vortices along the thermal gradient leads to a strong Nernst signal. The longitudinal voltage below T_c shows a nonlinear field dependence which indicates the feature of Abrikosov flux flow.

Above T_c, the dissipation may be caused by the motion of the spontaneously generated vortex-antivortex pairs. According to the theory derived by Berezinsky[17] and by Kosterlitz and Thouless[18] (BKT), just below a transition temperature T_{BKT} which lies very nearby T_c, in samples there are thermally excited vortices and antivortices binding in pairs, even in the absense of an external magnetic field. Above T_{BKT} the pairs unbind to form vortex plasma which can flow freely as pancake vortices with their cores confined inside individual superconducting layers. The possibility of this BKT transition was verified and studied in a layered HTS system.[19–25] In the region above T_c, the magnetic field applied on the samples influences the neutral vortices plasma and polarizes part of the vortices. The dissipation caused by vortex and antivortex on the tolal resistance is the same, although the moving directions of them are different. In other words, the dissipation resulted from the current driven vortex motion is not related to the polarization of, but to the total number of the vortex and the antivortex in the sample, which is constant when changing H. So the resistance of the sample in magnetic field above T_c is weakly dependent on the magnetic field as illustrated in Fig. 4. For the same reason, the longitudinal voltage induced by the motion of the vortex plasma in the normal state is also independent on the magnetic field.

In the case of Nernst effect a different consequence appears in the pseudogap region. The vortex plasma redirected by the external magnetic field moves across E-F along the thermal gradient, leading to the phase slips and a transverse Nernst electric field E_y appears consequently. The direction of the E_y caused by the vortex is different from that of the E_y caused by the antivortex moving along the same direction. So the direction and strength of E_y is not determined by the total number but by the amount of the difference between vortex and antivortex, i.e., by the sign and the amount of the net vortex. The density of the net vortex in the samples increases with increasing external magnetic field, leading to the increase of Nernst voltage with H in the field range of our experiment. The 2D feature of the Nernst effect in the pseudogap region of underdoped cuprate superconductors has been proven by the experiments of Wen *et al.*,[10] which supports our postulation above.

D. Manipulating vortex motion by thermal and Lorentz force

The Nernst signal and the longitudinal voltage as the result from the motion of vortex manipulated solely by the thermal gradient and solely by Lorentz force are discussed above. Now let us go on to discuss the result of manipulating the motion of the vortex by the thermal gradient and the Lorentz force together. With a transverse current applied along the A-B direction and a temperature gradient along the length direction of the $La_{1.89}Sr_{0.11}CuO_4$ single crystal at the same time, the voltage V_{EF} between the Nernst leads E and F are measured.

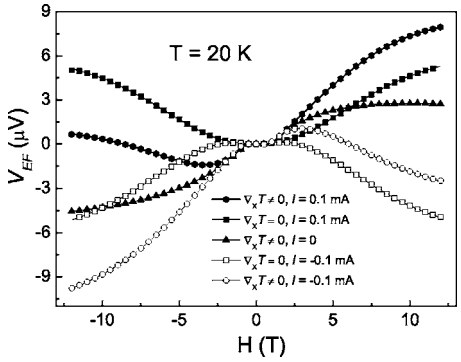

FIG. 7. The result of V_{EF} at the temperature of 20 K with/without a temperature gradient along the length direction and a transverse current along A-B on the $La_{1.89}Sr_{0.11}CuO_4$ single crystal. Different symbols represent the case of $I=0$ (closed triangles), $I=0.1$ mA (closed circles), $I=-0.1$ mA (open circles) with thermal gradient, and $I=0.1$ mA (closed squares) $I=-0.1$ mA (open squares), without thermal gradient. The heating power is 1.0 mW. For the convenience of comparison, all the curves have been shifted along the V_{EF} axis and the values of V_{EF} are zero when $H=0$ after the shift.

Figure 7 shows the result of V_{EF} at 20 K for the case $I=0$, $I=0.1$ mA, and $I=-0.1$ mA with and without thermal gradient. V_{EF} with thermal gradient and without current (presented by solid triangles) is the Nernst signal at this temperature, where we can see that the sign of V_{EF} is dependent on the direction of magnetic field. For the case of $\nabla_x T=0$ and $I\neq 0$, V_{EF} (closed and open squares) shows the characteristics of Abrikosov vortices and the sign of the V_{EF} after vortices melting is independent on the direction of current. The features of the curves are similar to those in Fig. 4. The results manipulating vortex motion by thermal and Lorentz force are shown in the case of $\nabla_x T\neq 0$ and $I=\pm 0.1$ mA (closed and open circles) in Fig. 7. All the curves show that the transport properties in mixed state are dominated by Abrikosov vortex motion.

Figure 8 shows the result at 80 K with the current of 0, 3, and −3 mA. In Fig. 8, all the curves have been moved along the V_{EF} axis and hence the values of V_{EF} are zero when $H=0$ for the convenience of comparison. The influence of the Faraday effects and the resistive components of the data are taken away by moving the curves. We can see from Fig. 8 that with positive transverse current, the V_{EF} measured under negative magnetic field is almost equivalent to the V_{EF} without current, but for the case under positive field, there is an obvious difference between the V_{EF} with current and that without current. With negative transverse current, the V_{EF} measured under positive magnetic field is almost equivalent to the V_{EF} without current, but for the case under negative

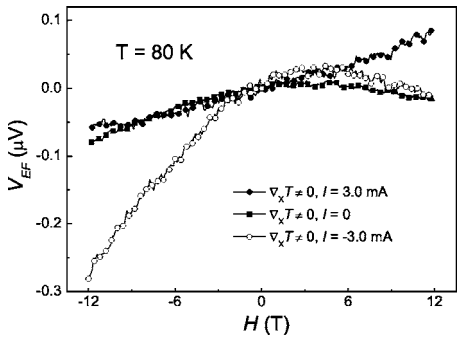

FIG. 8. The result of V_{EF} at the temperature of 80 K with a temperature gradient along the length direction and a transverse current along A-B on the $La_{1.89}Sr_{0.11}CuO_4$ single crystal. The closed squares, closed circles, and open circles present the case of 0, 3.0, and −3.0 mA, respectively. The heating power is 1.0 mW. All the curves have been vertically shifted to make the data comparable to that in Fig. 7.

field, there is an obvious difference between the V_{EF} with current and that without current. So we can conclude that the effects of the Lorentz force on the Nernst effect in the normal state are related to the direction of the magnetic field. This phenomenon cannot be explained by the effects of quasiparticles and may be explained only by the motion of vortex. So the Nernst signal above T_c is also contributed by flux motion, although the vortex structure and feature may be very different below and above T_c.

IV. CONCLUSIONS

The in-plane resistance, Nernst voltage, and longitudinal voltage in a new experimental configuration of the underdoped $La_{1.89}Sr_{0.11}CuO_4$ single crystal and optimally doped $YBa_2Cu_3O_{7-\delta}$ thin film are measured by sweeping magnetic field at fixed temperatures. The vortex motion is successfully manipulated by using thermal and/or Lorentz force in the mixed and normal states of the samples. The Nernst signal in the normal state is observed. The signal may be caused by the motion of quasiparticles or vortex or both. Our results indicate that Nernst signal above T_c may be contributed by vortex motion, though the contribution of the quasiparticle has not been excluded. Different vortices below and above T_c are expected if the strong Nernst signal in the pseudogap region was attributed to the vortex motion. Below T_c the dissipation is induced by the motion of the Abrikosov vortices. Above T_c the dissipation may be caused partly by the motion of the spontaneously generated unbinded vortex-antivortex pairs (vortices plasma).

ACKNOWLEDGMENTS

This work was supported by the National Natural Science Foundation of China (NSFC), the Ministry of Science and Technology of China (973 project No. 2006CB601002), and the Chinese Academy of Sciences.

*Electronic address: hhwen@aphy.iphy.ac.cn

[1] D. Pines, Physica C **235**, 113 (1994).
[2] V. J. Emery and S. A. Kievelson, Nature (London) **374**, 434 (1995).
[3] A. J. Millis, Nature (London) **398**, 193 (1999).
[4] V. J. Emery, S. A. Kivelson, and O. Zachar, Phys. Rev. B **56**, 6120 (1997).
[5] Ian Affleck and J. B. Marston, Phys. Rev. B **37**, 3774 (1988).
[6] Sudip Chakravarty, R. B. Laughlin, Dirk K. Morr, and Chetan Nayak, Phys. Rev. B **63**, 094503 (2001).
[7] Z. A. Xu, N. P. Ong, Y. Wang, T. Kakeshita, and S. Uchida, Nature (London) **406**, 486 (2000).
[8] Yayu Wang, Z. A. Xu, T. Kakeshita, S. Uchida, S. Ono, Yoichi Ando, and N. P. Ong, Phys. Rev. B **64**, 224519 (2001).
[9] Yayu Wang, N. P. Ong, Z. A. Xu, T. Kakeshita, S. Uchida, D. A. Bonn, R. Liang, and W. N. Hardy, Phys. Rev. Lett. **88**, 257003 (2002).
[10] H. H. Wen, Z. Y. Liu, Z. A. Xu, Z. Y. Weng, F. Zhou, and Z. X. Zhao, Europhys. Lett. **63**, 583 (2003).
[11] Yayu Wang, S. Ono, Y. Onose, G. Gu, Yoichi Ando, Y. Tokura, S. Uchida, and N. P. Ong, Science **299**, 86 (2003).
[12] Hiroshi Kontani, Phys. Rev. Lett. **89**, 237003 (2002).
[13] Iddo Ussishkin, S. L. Sondhi, and D. A. Huse, Phys. Rev. Lett. **89**, 287001 (2002).
[14] Shina Tan and K. Levin, Phys. Rev. B **69**, 064510 (2004).
[15] A. S. Alexandrov and V. N. Zavaritsky, Phys. Rev. Lett. **93**, 217002 (2004).
[16] F. Zhou *et al.*, Supercond. Sci. Technol. **16**, L7 (2003).
[17] V. L. Berezinsky, Zh. Eksp. Teor. Fiz. **59**, 907 (1970) [Sov. Phys. JETP **32**, 493 (1971)].
[18] J. M. Kosterlitz and D. J. Thouless, J. Phys. C **6**, 1181 (1973).
[19] Tomoko Ota, Ichiro Tsukada, Ichiro Terasaki, and Kunimitsu Uchinokura, Phys. Rev. B **50**, 3363 (1994).
[20] J. C. Culbertson, U. Strom, S. A. Wolf, and W. W. Fuller, Phys. Rev. B **44**, 9609 (1991).
[21] Y. Matsuda, S. Komiyama, T. Terashima, K. Shimura, and Y. Bando, Phys. Rev. Lett. **69**, 3228 (1992).
[22] A. K. Pradhan, S. J. Hazell, J. W. Hodby, C. Chen, Y. Hu, and B. M. Wanklyn, Phys. Rev. B **47**, 11374 (1993).
[23] L. Miu, G. Jakob, P. Haibach, Th. Kluge, U. Frey, P. Voss-de Haan, and H. Adrian, Phys. Rev. B **57**, 3144 (1998).
[24] S. Martin, A. T. Fiory, R. M. Fleming, G. P. Espinosa, and A. S. Cooper, Phys. Rev. Lett. **62**, 677 (1989).
[25] C. Capan, K. Behnia, J. Hinderer, A. G. M. Jansen, W. Lang, C. Marcenat, C. Marin, and J. Flouquet, Phys. Rev. Lett. **88**, 056601 (2002).